



Treating MTBE-contaminated water using sewage sludge-derived activated carbon

Musiliu A. Liadi¹ · Bassam Tawabini¹  · Reyad Shawabkeh² · Nabil Jarrah³ · Tajudeen A. Oyehan¹ · Abdulaziz Shaibani¹ · Mohammed Makkawi¹

Received: 15 April 2018 / Accepted: 6 July 2018 / Published online: 20 August 2018
© Springer-Verlag GmbH Germany, part of Springer Nature 2018

Abstract

In this study, sewage sludge-derived activated carbon (SDAC) was synthesized, characterized, and tested for its potential as an adsorbent of methyl tert-butyl ether (MTBE). The SDAC was produced by activating the sludge with zinc chloride and subsequently subjected to various ranges of pyrolytic temperatures. It was then characterized using SEM/EDX, BET, and TGA. The SEM-EDX analyses showed that impurities like Fe, Al, Mg, Mn, Ca, and Na of the raw sludge were removed by the higher pyrolytic temperature and acid-washing procedures. TGA showed the thermal stability of the produced material. Results of the BET revealed a significant increase in surface area of the sludge from 1.5 m²/g to 385 m²/g after acid washing. The MTBE removal efficiency of 70% was achieved after 60 min with 2 g/L of SDAC at pH 6, and initial MTBE concentration of 1 ppm. The adsorption kinetics of SDAC fitted into pseudo-second-order reactions. This work demonstrated a beneficial use of a bio-waste material (sewage sludge) in water treatment technologies.

Keywords Sewage sludge · Activated carbon · Characterization · Adsorption · MTBE

Introduction

Diverse options of sewage sludge disposal methods and utilization are available, ranging from land farming (Hejazi et al. 2003), landfilling, and road surfacing (Jarrah and Siddiqui 2012) as well as incineration (Nilsson and Dahlström 2005). Sewage sludge has also been utilized as components of starting materials in the making of lightweight aggregates usable in the geotechnics, gardening, and architectural design (Franus et al. 2016). In Saudi Arabia, the predominant sewage sludge disposal method is landfilling (Rio et al. 2006). Another sustainable and economical option for sludge disposal has recently

emerged which focuses on converting this solid waste into a useful carbonaceous adsorbent (Bagreev et al. 2001; Dai et al. 2014; Fang et al. 2010; Waqas et al. 2015). It has been reported that copious amounts of carbons, that can be thermally or chemically activated, are found in the sludge of biochemical origins (Martin et al. 2002; Julcour Lebigue et al. 2010). Chemical activation of sludge from sewage and dairy plants has been achieved with the use of chemical reagents like sulfuric acid, hydrochloric acid, potassium hydroxide, zinc chloride, etc., and the resulting adsorbents have been efficiently applied in wastewater treatment (Molina-Sabio et al. 1995; Shawabkeh et al. 2015; Sheha et al. 2013; Wu et al. 2005). Physical activation of sludge using steam had also been tested and the resulting activated carbons applied in pollutants' removal technology and toxic emission treatment (Rio et al. 2006).

In a recent work of Gu and his team (Gu et al. 2013), sewage sludge-derived activated carbon (SDAC) was applied for the adsorption of naphthalene dye intermediate using peroxide as oxidant. After 2-h treatment, a removal of 94% of 150 mg l⁻¹ of the dye was achieved. SDAC was also used to remove phenol and carbon tetrachloride (Chen et al. 2002). The adsorbent was found to have high adsorption capacities for both contaminants especially after been subjected to pyrolysis. Recently, Zhang and his research team applied SDAC produced with different

Responsible editor: Tito Roberto Cadaval Jr

✉ Bassam Tawabini
bassamst@kfupm.edu.sa

¹ Geosciences Department, King Fahd University of Petroleum and Minerals (KFUPM), P.O. Box 189, Dhahran 31261, Saudi Arabia

² Chemical Engineering Department, University of Jordan, Amman, Jordan

³ Chemical Engineering Department, Mutah University, Karak, Jordan

chemical activation reagents (H_2SO_4 , H_3PO_4 and ZnCl_2) in treating mercury-contaminated water (Zhang et al. 2005).

Methyl tert-butyl ether (MTBE) is popularly known as one of the groundwater pollutants and as a potential human carcinogen by USEPA (Squillace et al. 1997; Salimi et al. 2016). It has though been tentatively listed as a possible human carcinogen, its eco-toxicological health effects in lower animals and other marine biota have only been established (Shahidi Bonjar 2004; Shahidi and Ambigaipalan 2015). Conventional methods of treating MTBE-contaminated water, using an adsorbent, seem challenging as the analyte persists in the environment owing to its high-water solubility, high resistance to biodegradation and low adsorption rate onto the solid surface (Tawabini 2014). Therefore, enhancing these technologies for the removal of MTBE remains a priority for the researchers. Various illustrations of adsorbents tested for the removal of MTBE include fly ash, zeolite, granular activated carbon, bituminous activated carbon, activated carbon from coconut shell and modified oil sludge (Adebayo et al. 2016; Li et al. 2012; Shih et al. 2003; Zou et al. 2013). However, literature search revealed no previous work on utilizing SDAC for the removal of MTBE from contaminated water. This serves as a research gap to bridge and an investigation to explore.

Materials and methods

Materials

Samples of raw sewage sludge were collected from a wastewater treatment plant located in the city of Dhahran in the Eastern Province of Saudi Arabia. MTBE was purchased from Sigma-Aldrich with a purity of >99.8% (HPLC grade) was used for the study. Ultra-pure deionized water generated from a Milli-Q system was used in the preparation of stock solutions. Zinc chloride (ZnCl_2) pellet (99.99% from Panreac Quimica, Spain) was used for activation. Chemicals such as H_2SO_4 , HCl, and NaOH (lab grade) purchased from Chem-Lab NV, Belgium, were respectively used to adjust the pH of the solution. Nitrogen gas (99.99% purity) was used in the pyrolysis process of the sludge. Commercial activated carbon (GC-IPH, General Carbon Corporation, NJ) was also tested for its capacity to remove MTBE from water in comparison with the SDAC.

Preparation of SDAC

Raw sludge (RAW) samples were initially dried at 105 °C for 48 h, crushed into small particles and subsequently sieved to a size of < 500 μm . Chemical activation was then carried out by mixing the dried sludge with ZnCl_2 at a ratio of 1:2 and pyrolyzed afterwards under an inert atmosphere of nitrogen gas at a flow rate of 50 mL min^{-1} in a tubular furnace (ST-

1200RG-4, SuTong China) using a temperature of 700 °C, heating rate of 10 °C min^{-1} and a dwell time of 90 min. The carbonized granular SDAC (PYR) was then acid-washed with a liquid-solid ratio (L/S) of 20:1 at 80 °C using 0.5 M HCl and stirred for 6–7 h. Then, the acid treated SDAC was water-washed with deionized water (L/S ratio of 10:1 at 80 °C) several times until the pH of 6–7 was achieved. The liquid supernatant was then separated from the precipitates of activated carbon using a centrifuge (run at 3500 rpm for 15 min) and thereafter dried at 100 °C for 12 h. The dried activated carbon residue was referred to in this study as sludge derived activated carbon (SDAC). Finally, before testing its capacity to remove MTBE, the SDAC was characterized for its major properties.

Material characterization

The specific surface area and pore size distribution of the SDAC were respectively determined by adsorption of N_2 at 77 K using 2020 ASAP Micromeritics. The Brunauer-Emmett-Teller (BET) theory and Barret-Joyner-Halenda (BJH) method were employed for the specific surface area and pore size distribution characterization of the samples, respectively (Sethia and Sayari 2016). Thermogravimetric analysis (TGA) was conducted in a TA Instrument-Waters LLC, USA, at 20 °C min^{-1} and 50–60 ml min^{-1} of N_2 flow rate was employed for this work with about 7–10 mg of each of the four selected adsorbent material held on an alumina pan equipped with a heat regulator (furnace thermo-element). A dynamic temperature ramped at 10 °C per minute to 900 °C and Argon gas with a flow rate of 100 mL per min was adopted for this analysis. The surface morphological structure of all three states (RAW, PYR and SDAC) were analyzed by SEM-EDX (JOEL JSM 5900LV).

Zero point-of-charge (pH_{zpc}) of the SDAC was also conducted using pH probe. Certain portions of SDAC powder were introduced into a known volume (20 ml) of 0.1 mol/dm^3 KNO_3 solution. KNO_3 was selected as an inert electrolyte and the ionic strength was kept constant all along the experiments. Initial pH values (pH_i) of KNO_3 solution were adjusted from 3 to 11 by adding 0.1 M HNO_3 or KOH. The set up was left to equilibrate for 24 h in an isothermal shaker. The suspensions were filtered and the pH values (pH_f) were again measured using the ion-pH meter (Al-Qodah and Shawabkah 2009).

MTBE adsorption study

Several batch adsorption experiments were carried out using 40 ml of MTBE-spiked deionized water. For each run, different dosages SDAC were added to the spiked water containing some pre-determined levels of MTBE and thereafter tightly sealed to avoid any volatilization loss. The flasks were then placed on the shaker (Orbi-Shaker, Germany) for 220 min.

Several treatment parameters were tested including adsorbent doses (0.5–4 g/l), initial pH of solution (3–9), initial concentration of MTBE (500–4000 µg/l), a fixed agitation speed of 150 rpm and contact time of 30, 60, 90, 120 and 180mins. A few drops of 0.1 M of HCl or KOH were used to adjust the pH of the working solution. Following preparation of the stock solutions, the Thermo Scientific Trace GC Ultra gas chromatography/mass spectrometry (GC-MS) unit was calibrated to cover the range of concentrations to be used in the batch experiments (0.5 to 4000 µg/L). For all the concentration analyses, 1.0 mL of the solution was collected in a glass vial, centrifuged and analyzed. The ISQ single quadrupole mass spectrometer coupled Thermo Scientific Trace Gas chromatography unit, fitted with a Triplus Headspace injector unit and an auto-sampler was used for the analysis of the MTBE concentrations in the samples collected during the batch experiments. A DB 520.2 fused silica capillary gas chromatography column was used in the unit (60 m length; 0.32 mm internal diameter and 1.80 µm thickness). The stationary phase used was diphenyl dimethyl polysiloxane, while the carrier gas was helium, at a constant flow rate of 1.7 mL/min. The instrument configuration was programmed at a temperature of 50 °C for 1 min, ramped to 220 °C at a rate of 20 °C/min and held for 1.0 min. To volatilize the target analyte, incubation of the sample bearing vials was programmed to start at temperature rate of 80 °C per every 5 min in the auto-sampler, before the volatilized contents are taken by the syringe and injected into the unit. The electron ionization mode was utilized for the mass spectrometry unit (detector), having mass transfer line temperature of 200 °C and ion source temperature of 200 °C. Selected ion monitoring (SIM) mode was used to obtain the ion current at the mass to charge ratio of interest, having set the mass range of MTBE at 72.50–73.50. The amount of MTBE adsorbed per gram of adsorbent material (adsorption capacity (q_e) in mg/g) and its percentage removal are given in the Eqs. 1 and 2, respectively.

$$q_e = \frac{(C_0 - C_e)V}{W} \tag{1}$$

$$\%Removal = \frac{C_0 - C_e}{C_0} 100 \tag{2}$$

Where C₀ and C_e (mg/L) are the liquid-phase concentrations of MTBE at initial and equilibrium, respectively. V is the volume of the solution (L) and W is the mass of dry adsorbent used (g).

Adsorption equilibrium modeling and kinetics

Langmuir and Freundlich’s equations were adopted to assess the adsorption behavior of SDAC for MTBE removal from the aqueous medium.

Langmuir and Freundlich’s equations are as expressed below in their linearized forms:

$$q_e = \frac{q_m K_L C_e}{1 + K_L C_e} \tag{3}$$

Where q_e is the adsorbed amount at equilibrium (mg/g), C_e is the concentration of adsorbate at equilibrium (mg/l), q_m is the maximum adsorption capacity and K_L is the Langmuir constant related to the energy of adsorption (Shawabkeh and Abu-Nameh 2007), q_m and K_L can be deduced from the slope and intercept by plotting $\frac{C_e}{q_e}$ against C_e.

$$q_e = K_f C_e^{1/n} \tag{4}$$

Where C_e is the equilibrium MTBE concentration (mg/l); q_e is the amount of MTBE (mg) adsorbed per gram of the adsorbent at equilibrium (mg/g); K_f is the Freundlich adsorption constant related to the adsorbent adsorption capacity [(mg/g) (l/mg)^{1/n}]. A linear plot of logq_e against logC_e was used to obtain the values of K_f and n from the intercept and slope, respectively. Value of n should be in the range 1 to 10 to adapt this theorem for MTBE adsorption.

Adsorption kinetics demonstrates the solute uptake rate and as such represents the adsorption efficiency of adsorbents that can be explored in environmental pollution remediation technique (Lodeiro et al. 2006). A sample of 10 g/l dose of adsorbent was dissolved in 5 mg/L MTBE solution by shaking in an isothermal shaker at room temperature and the decreasing trend of concentration against sorption time (60, 90, 120, 180, 210, 255 and 300 min) was traced. The adsorption kinetics of MTBE was investigated with SDAC by employing two kinetic models namely: pseudo-first order and pseudo-second order are as presented below:

$$\log(q_e - q_t) = \log q_e - \frac{k_1}{2.303} t \tag{5}$$

$$\frac{t}{q_t} = \frac{1}{k_2 q_e^2} + \frac{t}{q_e} \tag{6}$$

where q_e and q_t are the amounts of MTBE adsorbed at equilibrium and at time t, respectively. k₁ is the rate constant of the pseudo-first-order adsorption process (min⁻¹) and k₂ is the rate constant of the adsorption pseudo-second-order model (g/mg/min). The values of k₁ for q_e in the pseudo-first-order model are respectively calculated from the slope and intercept of plots log(q_e - q_t) against t. Values of k₂ and q_e in the pseudo-second-order model are computed by a plot of $\frac{t}{q_t}$ versus t.

Results and discussion

Thermogravimetric analysis (TGA) properties of SDAC

The stacked curve of the TG analyses of the raw sludge (RAW), pyrolyzed and chemically activated SDAC (PYR)

and acid-washed chemically activated SDAC (ACD) is shown in Fig. 1. It can be observed that respective weight losses of about 13.4, 6.3, and 9.3% appear at 220, 110 and 114 °C for RAW, PYR, and final SDAC, respectively. The losses in weight at the stated points for the compared samples may be attributed to the loss of the adsorbed water. As displayed in TG curve, a large weight loss of about 40% appears at 220–470 °C temperature range for RAW is attributed to the volatilization/decomposition of the volatiles, inorganic and organic substance.

The smaller weight loss obtainable for PYR and SDAC (5%) is an evidence of the effective pyrolytic and acid-washing step employed in the production of SDAC. Some organics were burnt off during the pyrolytic process and those that resisted this were eventually washed off along with the existing inorganic substances by the subsequent acid-washing SDAC treatment. About 19% weight loss observed for RAW in the range of 470–900 °C is attributed to the generation of gas like CO₂ and CO. There is no appreciable weight loss between 600 and 900 °C for RAW thus the temperature ranges 470–900 °C is deemed as the most significant for pyrolysis. PYR and SDAC curves do not possess a distinct temperature gradation as does the RAW. The gas evolution stage may not appear in the processed samples as the ZnCl₂ used for activation might have reacted with some organics and therefore burnt off during the process. The activation, pyrolysis and acid-washing processes help in creating some nascent pores in the sludge and ultimately lead to the formation of –OH, necessary for adsorption in the SDAC. TGA results indicate that the final SDAC material is more thermally stable than RAW and PYR materials. Examining the thermal properties of sludge alongside with the two processed samples (PYR and SDAC) helps in an in-depth understanding of the influence of thermal treatment on surface features and pore structures.

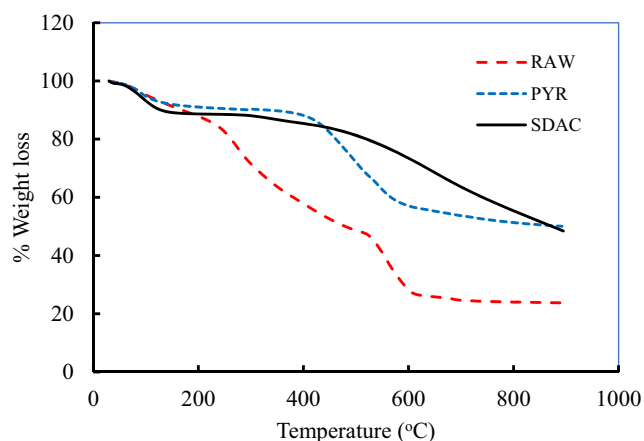


Fig. 1 TG analyses of the RAW, PYR and SDACs

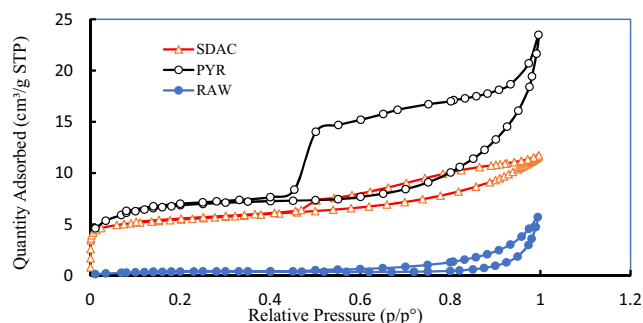


Fig. 2 Adsorption-desorption isotherms for N₂ at 77 K determined for RAW, PYR and SDAC

BET analysis of SDAC materials

Figure 2 shows the nitrogen (N₂) adsorption isotherms determined at 77 K for RAW, PYR, and SDAC materials. It can be observed that the amount of N₂ adsorbed is low for all the three samples. However, the N₂ adsorption capacities of the two biochars (PYR and SDAC) were larger than that of the raw sludge (RAW). In accordance with IUPAC classification, the three samples in question exhibit type IV isotherms. Appreciable adsorption was observed at high relative pressure (p/p^0) values between 0.9 and 1.0 which are suggestive of the presence of meso-porosity. Some of the textural parameters derived from the N₂ isotherms are presented in Table 1. The specific surface area values were respectively 1.5 m²/g, 21.7 m²/g and 385 m²/g for RAW, PYR and SDAC. The increase in surface area was 18 times more due to pyrolysis and 257 times more due to combined effects of pyrolysis and acid washing. The micro-porosity, and by extension BET surface area, increases dramatically under the influence of pyrolysis and combined effect of acid washing and pyrolysis from 1.5 for RAW to 21.7 and 385 m²/g respectively. These results were in line with the earlier works of Bagreev and Badosz (2002) and Molina-Sabio et al. (1995). However, other authors reported that solid products derived from sewage sludge pyrolysis were highly macro-porous with relatively low meso and micro-pore areas independently of pyrolytic conditions (Lu et al. 2013). The nascence of meso-porosity during activation is affirmed by hysteresis loops seen for all the three samples. Hysteresis loops are the resultant effects of the variation in the mechanisms of meso-pore filling and emptying during capillary condensation and evaporation of adsorbing molecules, respectively.

Figure 3 shows the plot of cumulative pore volume against pore diameter of RAW, PYR and SDAC. Although a pronounced cumulative pore volume is obtainable for SDAC, all the three samples possess similar shapes. A substantial change in pore size distribution was observed with the combined effect of pyrolysis and acid washing. The ultimately generated adsorbent (SDAC) generally has the largest volume of meso-pores and the least pore size width (Table 1).

Table 1 Textural properties obtained from N₂ adsorption isotherms of RAW, PYR and SDAC (SB = BET surface area, Se (external pore area), Sm = Microporous size, Vt = Total pore volume, Vm = Micropores' volume, Vme = meso-pore's volume Dp = Average pore diameter)

Samples	S _B (m ² /g)	Se (m ² /g)	% S _B	Sm (m ² /g)	%S _B	Vt (cm ³ /g)	Vm < 20 Å (cm ³ /g)	Vme < 500 Å (cm ³ /g)	Dp (Å)
RAW	1.54	1.47		0.07	4.36	95.64	Nil	0.00	120.71
PYR	21.70	11.60	53.45	10.10	46.55	0.03	0.01	0.03	66.96
SDAC	385.07	171.71	44.59	213.37	55.41	0.36	0.12	0.25	37.52

SEM/EDX characterization of SDAC materials

To further understand the various changes in the mineral phases and surface morphology of the adsorbent in question and to assess the effect of acid washing in the production process, the SEM images of RAW, PYR and SDAC were taken at magnifications of 50 and 100 kX as depicted in Fig. 4a–f. SEM micrographs (Fig. 4a–b) show that the RAW materials are somewhat compacted, fibrous, bumpy, crumb and agglomerate structure with sprays of some grayish particles while the PYR material (Fig. 4c–d) consists of sparingly dispersed flaky particle, minerals and probably some highly conjugated aromatic and aliphatic compounds that may be main factors to adsorbents' variation in surface charge and functional groups. On the other hand, Fig. 4e–f shows images of the conspicuous, largely amorphous and fine granular particles with the dimension varied from 500 to 1000 nm. The release of volatile matter and washing away of the inorganic matters could be the reasons for having more cracks and pores in SDAC much more than PYR and RAW.

Energy dispersive X-ray (EDX)

The elemental composition of the adsorbent material and the effect of acid washing adopted in the production process are better understood by EDX spectroscopy. Figure 5a–d shows the EDX spectra of both PYR and SDAC. EDX spectroscopy revealed the qualitative and quantitative measure of the existing metal impurities occurring in PYR in form of elemental

composition. Alkali and Alkali earth metals like K, Ca, Al, Mg, Zn, Fe, Si, and non-metallic elements like C, O, Cl, P, S were respectively found as feldspar, Wollastonite, bauxite, magnesium oxide, zinc metal, iron, silica, limestone, potassium chloride, gallium phosphate and sulphates. The elements' respective abundances (represented in percentages by weight and by atom) are as presented in Fig. 5. The effectiveness of washing the adsorbents with nitric acid was evident in the EDX spectra shown in the Figure due to the removal of many elements (impurities). Virtually all metals, non-metals and other impurities that can serve as potential sources of cross-contamination of the aqueous solution were significantly removed from the adsorbent except for carbon, oxygen and scantily available silicon.

Batch adsorption runs for the removal of MTBE

Effect of adsorbent dose on MTBE adsorption

To study the impact of adsorbent dosage on the adsorption of MTBE, five different dosages of each SDAC and CAC were measured and assessed for their adsorption capacity and removal efficiency. The treatment parameters; agitation speed, pH, time, temperature and initial concentration, were respectively fixed at 150 rpm, pH 6, 60 min, room temperature and 1 ppm. In Fig. 6a, the overall removal efficiency and adsorptive capacity of both adsorbents increased with increasing dosage rate. CAC's maximum absorption potential of about 70% was obtained at the dosage rate of 1 g/L. It can also be observed that the optimum removal efficiency of 70% for CAC and SDAC was respectively reached at 1 g/L and 2 g/L of the respective adsorbents. Figure 6b, the highest obtainable adsorptive capacities of the adsorbents were respectively 1200 µg/g and 900 µg/g for CAC and SDAC. The availability of more binding sites owing to the increase in adsorption surface can be a plausible explanation for the increase in MTBE removal efficiency. This observation is in line with the previous works of Rengaraj (Rengaraj et al. 2002) that investigated the phenol's adsorptive tendency on rubber seed coat, and Shah et al. (2015) who researched on iron impregnated activated carbon as an efficient adsorbent for the removal of Methylene Blue and much more recently Ganiyu et al. (2016) who studied the influence of aluminum impregnation on activated carbon for enhanced desulfurization of DBT at ambient temperature.

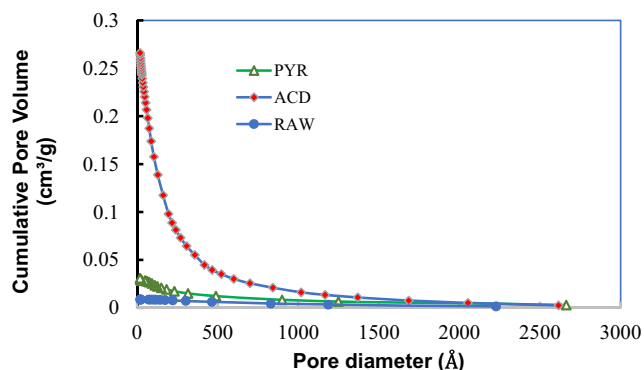


Fig. 3 Cumulative pore volumes versus pore diameter for RAW, PYR and SDAC

Fig. 4 SEM micrographs of the RAW (a–b), the PYR (c–d), and the SDAC (e–f)

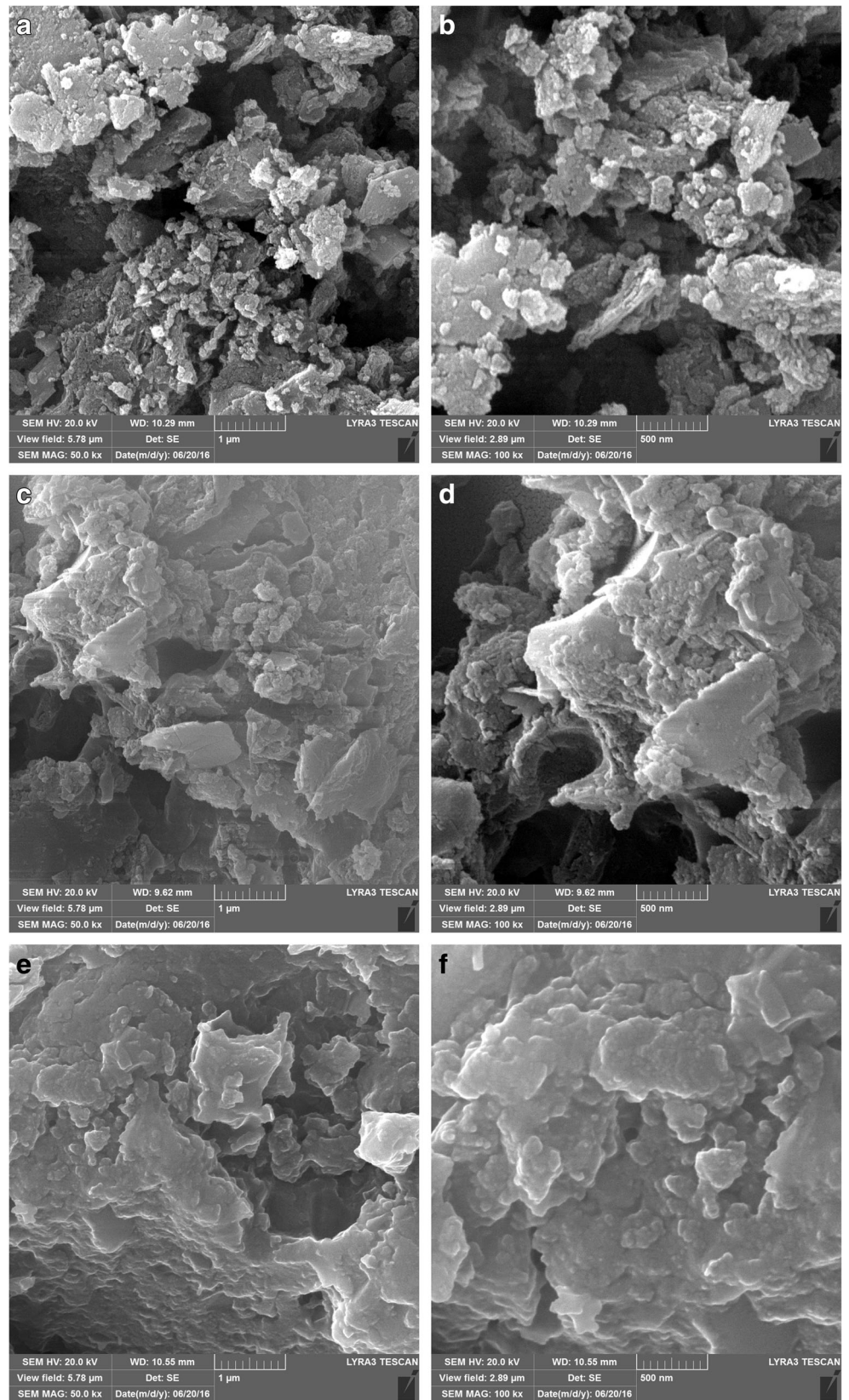
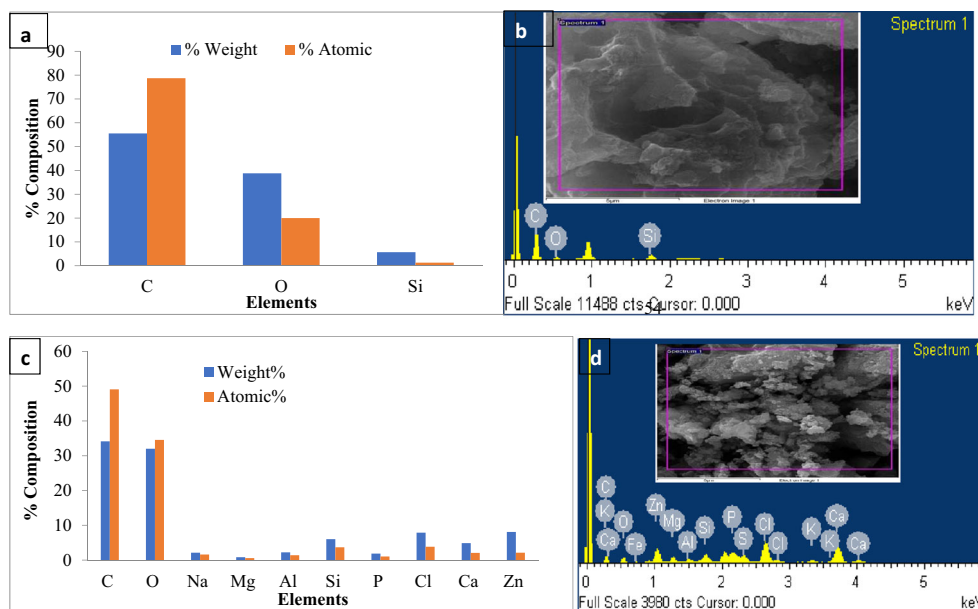


Fig. 5 EDX elemental particle analysis of PYR (a and b) and SDAC (c and d)



Effect of solution pH on MTBE adsorption

The pH of the solution is one of the main factors employed to explain the adsorbent’s surface charge and extent of ionization of the target analytes in solution. The adsorption of MTBE by the SDAC and CAC at various pH values of 3–9 for the fixed

initial MTBE concentration of 1 ppm, agitation speed of 150 rpm, contact time of 60 min, constant room temperature and an adsorbent dosage of 2 g/L was investigated and results are presented in Fig. 7.

A remarkable variation in MTBE adsorption behavior under different variable conditions of pH is observed for the SDAC and CAC. It is noticed that the MTBE removal efficiencies increased with increasing pH values. Again, MTBE adsorptive behavior of the adsorbent in question was found to be optimum at pH 6 with a recorded MTBE removal efficiency of 45%. This may be due to the protonation and/or polarization of ether under acidic condition, which facilitated the severance of MTBE from water. For CAC, MTBE removal efficiencies rose with increasing pH levels. The optimum pH range with the highest removal efficiency was found to be between 5 and 6 with a recorded removal of 65%. CAC at all levels of pH displayed a favorable and better adsorptive behavior for MTBE than SDAC (except at pH 6 where the latter outperforms the former).

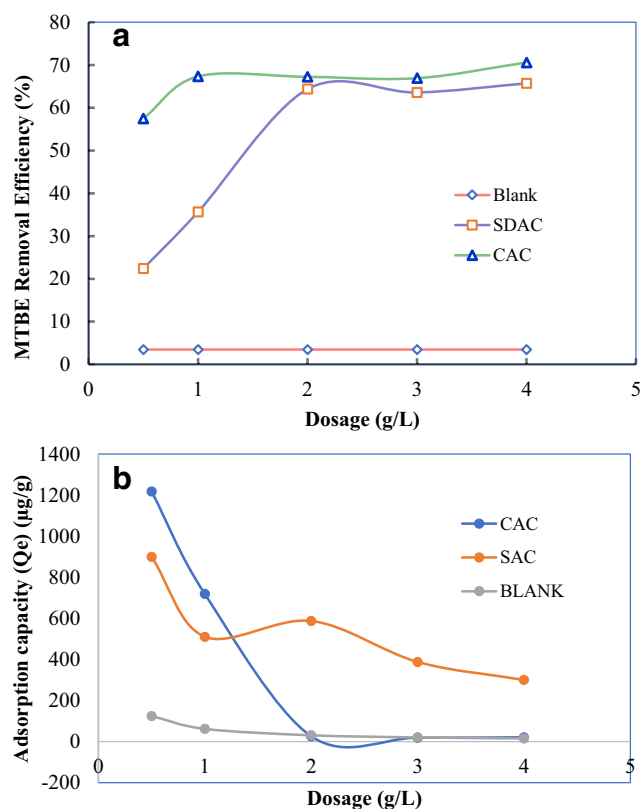


Fig. 6 (a) Effect of adsorbent dosage on MTBE removal efficiency by CAC, SDAC and BLANK. (b) Effect of adsorbent dosage on adsorptive capacity of CAC, SDAC and BLANK

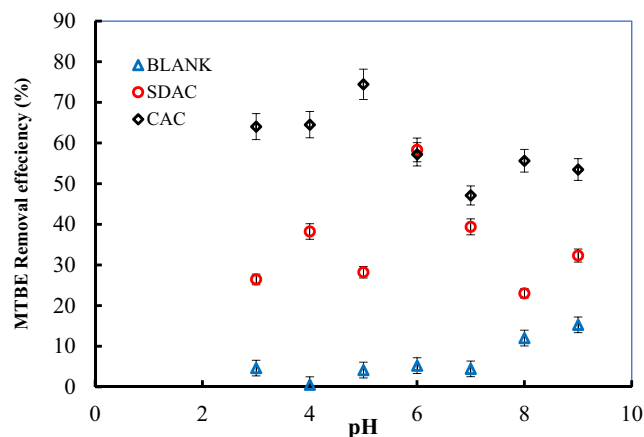


Fig. 7 Effect of pH on MTBE removal by SDAC, CAC and Blank

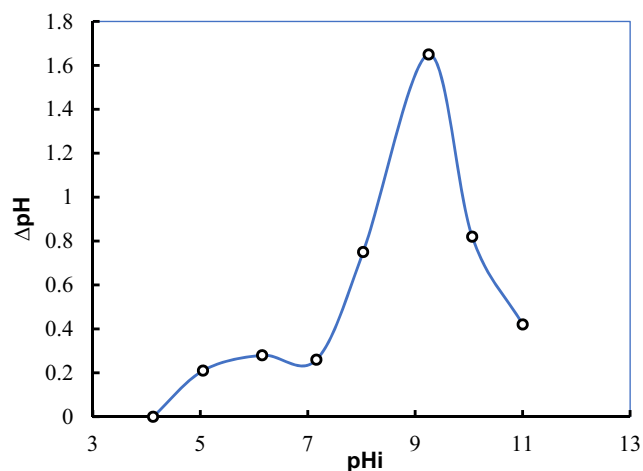


Fig. 8 Zero point-of-charge, pHzpc, for SDAC samples

Moreover, Fig. 8 shows the pHzpc of the adsorbent to be 7.16—a practically zero point of charge. ZPC describes the condition when the electrical charge density on the surface of the adsorbent is zero. It is usually determined in relation to an electrolyte’s pH, and the zpc value is assigned to a given substrate, adsorbent or colloidal particle. Batch equilibrium technique was employed to establish pHzpc of the SDAC powder. Generally, adsorbent’s surface is either positively or negatively charged (Selmani et al. 2015). The charge distribution pattern will be solely based on adsorbent-analyte surface interaction. If the pH of the solution is high enough, the surface becomes negatively charged and the positive ions from the solution (solute) will be attracted to the surface through electrostatic forces while the anions will be attracted at pH lower than the surface zpc. This means that SDAC can work at neutral pH without the need to adjust the pH as a pre-treatment step. It can, therefore, be concluded that the optimum pH 6 (a very weak acidic to neutral pH value) favors the MTBE removal efficiency of SDAC whose characteristic zpc is neutral.

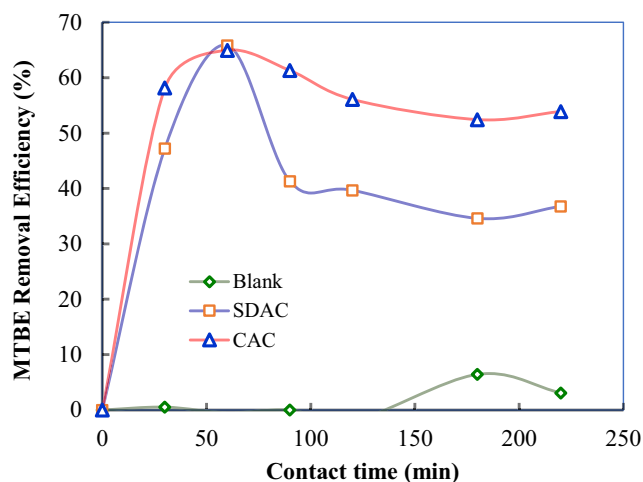


Fig. 9 Effect of contact time on MTBE adsorption behavior of SDAC and CAC

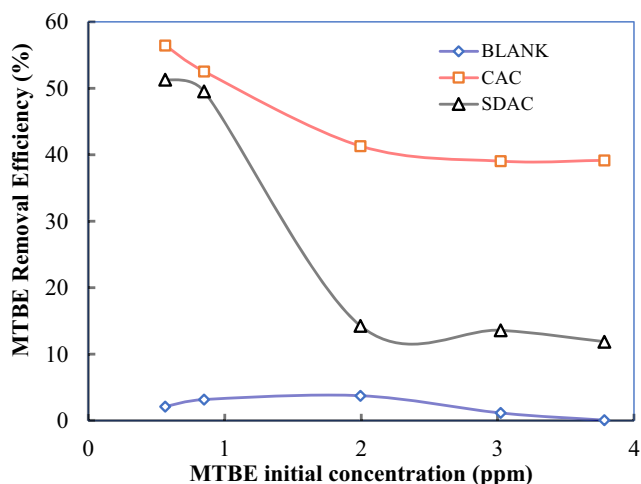


Fig. 10 Effect of initial MTBE concentration on removal efficiency by CAC and SDAC

Effect of contact time on MTBE adsorption

The effect of contact time in the adsorption process is shown in Fig. 9. The adsorbent-adsorbate nature of interaction dictates the optimum contact time for the maximum removal efficiency. The efficiency of MTBE removal by SDAC for different contact times was investigated. In the experiments, optimum pH 6, initial MTBE concentration of 1 ppm, adsorbent dosage rate of 2 g/L and equilibrium time ranging from 30 to 220 min were employed with a fixed agitation speed of 150 rpm. The adsorption of MTBE by SDAC and CAC was found to increase with time till 60 min of contact time after which there was a gradual decline in the adsorption. This observation can be explained by the adsorption equilibrium phenomenon, in which the rate of adsorption was greater than the rate of desorption until the optimum contact time of 60 min, in which the adsorption sites on the adsorbent were saturated. Beyond this point, the rate of desorption was greater than the rate of adsorption, accounting for the slight and gradual decline in the MTBE adsorption beyond the optimum time of 60 min. Li et al. also

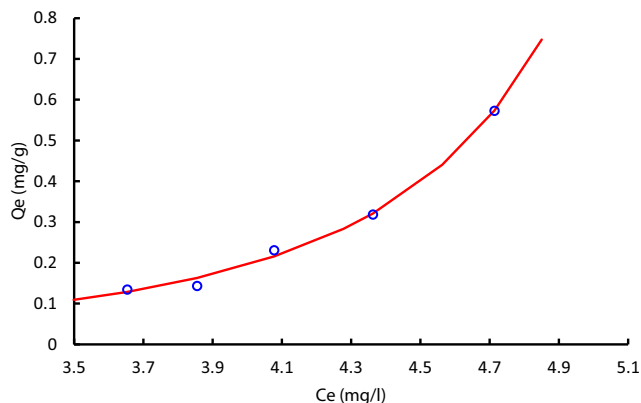
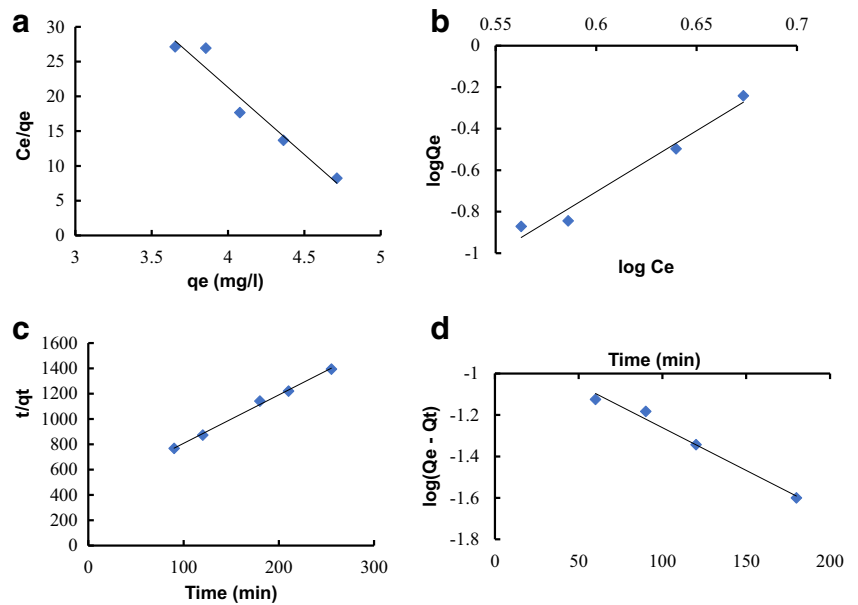


Fig. 11 Graph of adsorptive capacity of the SDAC (Q_e) vs equilibrium concentration of MTBE (C_e)

Fig. 12 (a) Linearized Langmuir isotherms for MTBE adsorption. (b) Linearized Freundlich isotherms for MTBE adsorption. (c) Pseudo-second-order sorption kinetics of MTBE. (d) Pseudo-first-order sorption kinetics of MTBE



reported 10% desorption upon the use of modified oil sludge (MOS) for MTBE removal from aqueous solution (Li et al. 2012).

Effect of initial MTBE concentration on adsorption

With respect to the nature of the adsorbent-adsorbate interaction, there is generally a decrease in the removal efficiency of the adsorbents as the concentration of the solute/adsorbate increases. The decrease in adsorbent’s adsorptive tendency is usually linked to the saturation of the binding sites (Salleh et al. 2011). This study also relatively depicted the same trend for adsorption behavior of both adsorbents in question. Figure 10 summarizes the influence of initial concentrations of MTBE on the removal efficiencies and adsorptive capacities of the two adsorbents (SDAC and CAC) while fixing all other parameters. It can be observed that the highest obtainable removal efficiency for both adsorbents (57% for CAC and 51% for SDAC) was at the smallest concentration of 0.5 ppm. The removal dropped gradually in CAC by 10% at

1 ppm concentration and by 17% at other concentrations. Initial concentrations 0.5 and 1 ppm seemed favorable for adsorption in SDAC also, as there was a little drop in the removal from these two concentrations. The plausible explanation for this observation was that at low concentration, adsorbates have enough unsaturated active sites in the adsorbents to bind with and at higher concentrations when more and more of the adsorbates are available in the solution, the active bind sites receive the adsorbate until they reach the saturation point (Senthil Kumar et al. 2010).

Adsorption isotherms

The graph showing the linear relationship between the adsorptive capacity of the adsorbent and the equilibrium concentrations of the MTBE is as shown in Fig. 11. The linearized adsorption isotherms of MTBE for Freundlich and Langmuir models are presented in the Fig. 12a and b and their corresponding isotherm parameters are summarized in Table 2. From the correlation coefficients (Table 2), Freundlich

Table 2 Freundlich and Langmuir adsorption isotherm parameters of MTBE adsorption comparison of SDAC and other adsorbents

Solute	Adsorbent	Freundlich			Langmuir			Reference
		K_f	N	R^2	q_m (mg/g)	K_L (L mg ⁻¹)	R^2	
MTBE	¹ SDAC	5.76E-5	0.1600	0.9712	0.500	0.2005	0.9687	This work
	² MOS	231.8	1.23	0.93	NA	NA	NA	(Shahidi Bonjar 2004)
	³ MFA	0.514	17.83	0.783	0.48	-1.2472	0.9875	(Ji et al. 2009)
	⁴ CMP	NA	NA	NA	2.18	0.118	0.9771	(Ji et al. 2009)
	⁵ NPP	NA	NA	NA	14.8	0.076	0.9851	(Ji et al. 2009)

¹ Sewage sludge-derived activated carbon, ² modified oil sludge, ³ modified fly ash, ⁴ chromomethylated polymer, ⁵ non-polar porous polymer

Table 3 Kinetic parameters for the adsorption of MTBE and other adsorbents compared

Solute	Sample	Pseudo-first-order			Pseudo-second-order			Reference
		q_e (mg/g)	K_1 (min ⁻¹)	R^2	q_e (mg/g)	K_2 (g mg ⁻¹ min ⁻¹)	R^2	
MTBE	SDAC	0.1416	9.44×10^{-3}	0.9832	2.26	3.52×10^{-2}	0.996	This work
	CMP	NA	NA	NA	2.28	4.33×10^{-2}	0.999	(Ji et al. 2009)
	NPP	NA	NA	NA	8.28	6.21×10^{-3}	1	(Ji et al. 2009)
	PCP	NA	NA	NA	19.62	3.07×10^{-4}	0.998	(Ji et al. 2009)

Chromo-methylated polymer, CMP; non-porous polar polymer, NPP; and post cross-linked polymer, PCP compared with SDAC

equation with correlation coefficient value of 0.9712 fitted the data for MTBE adsorption which is better than that of Langmuir's (0.9687) (Fig. 12a and b). Again, the amount of MTBE (in mg) adsorbed by 1 g of SDAC and MFA; (adsorption capacity) seemed to be the lowest among all other adsorbents compared in Table 2. The respective adsorption capacities in mg/g for NNP, CMP, SDAC and MFA are 14.4, 2.18, 0.5 and 0.48. This suggests that our adsorbent's adsorption capacity needs to be improved upon. Freundlich isotherm for MTBE adsorption assumes the exponential distribution of adsorption sites and energies and the multilayer adsorption of solute occurs on the heterogeneous surfaces (Yu et al. 2005). This also justifies the results of the SEM images taken for the SDAC. The surface morphology of the adsorbent was revealed to be an amorphous, heterogeneous surface with relatively larger BET surface area.

Adsorption kinetics

Figure 11 shows the linearized data for the sorption capacity, time and the pseudo-second-order kinetic plots. The kinetic parameters of SDAC are presented in Table 3. The correlation coefficient values (R^2) for both orders of reaction are above 0.97 and the fitting curves are all well linearized. The pseudo-first-order reaction's data are not available for the polymers (chromo-methylated polymer; CMP, non-porous polar polymer; NPP, and post cross-linked polymer; PCP) compared with the SDAC in Table 3. Of all the adsorbents compared, SDAC, though with a lower adsorption capacity, was the second in the list to have a faster adsorption rate constant of 3.52×10^{-2} g mg⁻¹ min⁻¹ after chromo-methylated polymer. This may be attributed to a moderate average pore width of the microporous size which allows MTBE to intra-diffuse.

Conclusion

The main tasks of this work were the synthesis of green adsorbent from a bio-waste—sewage sludge—and its subsequent application in treating the MTBE-contaminated water.

The adsorbent produced was characterized, prior to exploring its potentials for MTBE removal, using FESEM, EDX, FTIR, TGA and BET. The results of the characterization suggest that SDAC has a porous surface of 385 m²/g. The removal efficiency of 70% was achieved while using the produced adsorbent-SDAC, for the removal under the experimental conditions of 2 g/L dose, pH 6, agitation speed of 150 rpm, and initial MTBE concentration of 1 ppm. The adsorption isotherm and kinetics are better represented respectively by Freundlich model and pseudo-second-order reaction owing to their higher correlation coefficients. In adsorption technology, it is environmentally sustainable and cost effective to utilize adsorbent produced from sludge.

Acknowledgements The authors acknowledge King Fahd University of Petroleum & Minerals (KFUPM) for providing an enabling environment, necessary tools and financial support to carry out this study.

Nomenclature C_t (mg/l), Equilibrium concentration of MTBE at time t ; C_e (mg/l), Equilibrium concentration of MTBE obtained at the end of experiment.; C_0 (mg/L), Initial concentration of MTBE, (mg/l).; D_p (Å), Average pore diameter.; K_f , Freundlich isotherm constant; K_L (L/mg), Langmuir constant related to the energy of adsorption.; m (g), mass of the adsorbed sample; q_e (mg/g), Amount of MTBE adsorbed per unit mass of adsorbent at equilibrium.; q_t (mg/g), Amount of MTBE adsorbed at a given time.; q_m (mg/g), Maximum adsorption capacity of MTBE per unit mass of adsorbent.; S_B (m²/g), BET surface area of the adsorbent; S_e (m²/g), External pore surface area; t (min), Time of running the isotherm experiment; V (mL), Volume of the solution.; V_m (cm³/g), Micropores volume; V_t (cm³/g), Total pore volume

References

- Adebayo SB, Tawabini BS, Atieh MA, Abulilaiwi FA, Alfadul S (2016) Investigating the removal of methyl tertiary butyl ether (MTBE) from water using raw and modified fly ash waste materials. *Desalin Water Treat* 57:26307–26312
- Al-Qodah Z, Shawabkah R (2009) Production and characterization of granular activated carbon from activated sludge. *Braz J Chem Eng* 26:127–136
- Bagreev A, Bandosz TJ (2002) H₂S adsorption/oxidation on materials obtained using sulfuric acid activation of sewage sludge-derived fertilizer. *J Colloid Interface Sci* 252:188–194

- Bagreev A, Bandosz TJ, Locke DC (2001) Pore structure and surface chemistry of adsorbents obtained by pyrolysis of sewage sludge-derived fertilizer. *Carbon* 39:1971–1979
- Chen X, Jeyaseelan S, Graham N (2002) Physical and chemical properties study of the activated carbon made from sewage sludge. *Waste Manag* 22:755–760
- Dai W, Gong R, Hu J, Zhou L-M (2014) Thiophene capture by an oxidation-modified activated carbon derived from bergamot. *Sep Sci Technol* 49:367–375
- Fang P, Cen C, Chen D, Tang Z (2010) Carbonaceous adsorbents prepared from sewage sludge and its application for Hg⁰ adsorption in simulated flue gas. *Chin J Chem Eng* 18:231–238
- Franus M, Barnat-Hunek D, Wdowin M (2016) Utilization of sewage sludge in the manufacture of lightweight aggregate. *Environ Monit Assess* 188:10–15
- Ganiyu SA, Alhooshani K, Sulaiman KO, Qamaruddin M, Bakare IA, Tanimu A, Saleh TA (2016) Influence of aluminium impregnation on activated carbon for enhanced desulfurization of DBT at ambient temperature: role of surface acidity and textural properties. *Chem Eng J* 303:489–500
- Gu L, Zhu N, Guo H, Huang S, Lou Z, Yuan H (2013) Adsorption and Fenton-like degradation of naphthalene dye intermediate on sewage sludge derived porous carbon. *J Hazard Mater* 246-247:145–153
- Hejazi RF, Husain T, Khan FI (2003) Landfarming operation of oily sludge in arid region—human health risk assessment. *J Hazard Mater* 99:287–302
- Jarrah RT, Siddiqui MK (2012) Sustainability: opportunities and challenges from a construction contractor's perspective, ICSDEC 2012: developing the frontier of sustainable design, engineering, and construction. American Society of Civil Engineers, Fort Worth
- Ji B, Shao F, Hu G, Zheng S, Zhang Q, Xu Z (2009) Adsorption of methyl tert-butyl ether (MTBE) from aqueous solution by porous polymeric adsorbents. *J Hazard Mater* 161:81–87
- Julcour Lebigue C, Andriantsiferana C, N'Guessan K, Ayrat C, Mohamed E, Wilhelm A-M, Delmas H, Le Coq L, Gerente C, Smith KM, Pullket S, Fowler GD, Graham NJD (2010) Application of sludge-based carbonaceous materials in a hybrid water treatment process based on adsorption and catalytic wet air oxidation. *J Environ Manag* 91:2432–2439
- Li YH, Liu YL, Deng H, Zhang SL (2012) The adsorption and desorption characteristics of a novel sorbent in groundwater remediation: modified oil sludge. In: Cheng GZAS (ed) *Advanced Materials Research*, pp 412–417
- Lodeiro P, Barriada JL, Herrero R, Sastre de Vicente ME (2006) The marine macroalga *Cystoseira baccata* as biosorbent for cadmium(II) and lead(II) removal: kinetic and equilibrium studies. *Environ Pollut* 142:264–273
- Lu H, Zhang W, Wang S, Zhuang L, Yang Y, Qiu R (2013) Characterization of sewage sludge-derived biochars from different feedstocks and pyrolysis temperatures. *J Anal Appl Pyrolysis* 102: 137–143
- Martin MJ, Adriana A, Dolores BM, Miquel R (2002) Towards waste minimisation in WWTP: activated carbon from biological sludge and its application in liquid phase adsorption. *J Chem Technol Biotechnol* 77:825–833
- Molina-Sabio M, RodRíguez-Reinoso F, Caturla F, Sellés MJ (1995) Porosity in granular carbons activated with phosphoric acid. *Carbon* 33:1105–1113
- Nilsson C, Dahlström H (2005) Treatment and disposal methods for wastewater sludge in the area of Beijing, China. Lund University, Sweden
- Rengaraj S, Moon S-H, Sivabalan R, Arabindoo B, Murugesan V (2002) Removal of phenol from aqueous solution and resin manufacturing industry wastewater using an agricultural waste: rubber seed coat. *J Hazard Mater* 89:185–196
- Rio S, Le Coq L, Faur C, Lecomte D, Le Cloirec P (2006) Preparation of adsorbents from sewage sludge by steam activation for industrial emission treatment. *Process Saf Environ Prot* 84:258–264
- Salimi A, Vaghar-Moussavi M, Seydi E, Pourahmad J (2016) Toxicity of methyl tertiary-butyl ether on human blood lymphocytes. *Environ Sci Pollut Res* 23:8556–8564
- Salleh MAM, Mahmoud DK, Karim WAWA, Idris A (2011) Cationic and anionic dye adsorption by agricultural solid wastes: a comprehensive review. *Desalination* 280:1–13
- Selmani A, Špadina M, Plodinec M, Delač Marion I, Willinger MG, Lützenkirchen J, Gafney HD, Redel E (2015) An experimental and theoretical approach to understanding the surface properties of one-dimensional TiO₂ nanomaterials. *J Phys Chem C* 119:19729–19742
- Senthil Kumar P, Ramalingam S, Senthamarai C, Niranjanaa M, Vijayalakshmi P, Sivanesan S (2010) Adsorption of dye from aqueous solution by cashew nut shell: studies on equilibrium isotherm, kinetics and thermodynamics of interactions. *Desalination* 261:52–60
- Sethia G & Sayari A (2016) Activated carbon with optimum pore size distribution for hydrogen storage. *Carbon* 99:289–294
- Shah I, Adnan R, Wan Ngah WS, Mohamed N (2015) Iron impregnated activated carbon as an efficient adsorbent for the removal of methylene blue: regeneration and kinetics studies. *PLoS One* 10: e0122603
- Shahidi F, Ambigaipalan P (2015) Phenolics and polyphenolics in foods, beverages and spices: antioxidant activity and health effects—a review. *J Funct Foods* 18:820–897
- Shahidi Bonjar GH (2004) Potential ecotoxicological implication of methyl tert-butyl ether (MTBE) spills in the environment. *Ecotoxicology* 13:631–635
- Shawabkah R, Al-Qodah Z, Al-Bsoul A (2015) Bio-adsorption of triadimenol pesticide from aqueous solutions using activated sludge of dairy plants. *Desalin Water Treat* 53:2555–2564
- Shawabkeh RA, Abu-Nameh ESM (2007) Absorption of phenol and methylene blue by activated carbon from pecan shells. *Colloid J* 69:355–359
- Sheha D, Khalaf H, Daghestani N (2013) Experimental design methodology for the preparation of activated carbon from sewage sludge by chemical activation process. *Arab J Sci Eng* 38:2941–2951
- Shih TC, Wangpaichitr M, Suffet M (2003) Evaluation of granular activated carbon technology for the removal of methyl tertiary butyl ether (MTBE) from drinking water. *Water Res* 37:375–385
- Squillace PJ, Pankow JF, Korte NE, Zogorski JS (1997) Review of the environmental behavior and fate of methyl tert-butyl ether. *Environ Toxicol Chem* 16:1836–1844
- Tawabini BS (2014) Simultaneous removal of MTBE and benzene from contaminated groundwater using ultraviolet-based ozone and hydrogen peroxide. *Int J Photoenergy* 2014:7
- Waqas M, Li G, Khan S, Shamshad I, Reid BJ, Qamar Z, Chao C (2015) Application of sewage sludge and sewage sludge biochar to reduce polycyclic aromatic hydrocarbons (PAH) and potentially toxic elements (PTE) accumulation in tomato. *Environ Sci Pollut Res* 22: 12114–12123
- Wu F-C, Tseng R-L, Juang R-S (2005) Preparation of highly microporous carbons from fir wood by KOH activation for adsorption of dyes and phenols from water. *Sep Purif Technol* 47:10–19
- Yu L, Adams C, Ludlow D (2005) Adsorption isotherms for methyl tert-butyl ether and other fuel oxygenates on two bituminous-coal activated carbons. *J Environ Eng* 131:983–987
- Zhang F-S, Nriagu JO, Itoh H (2005) Mercury removal from water using activated carbons derived from organic sewage sludge. *Water Res* 39:389–395
- Zou J, Dai Y, Wang X, Ren Z, Tian C, Pan K, Li S, Abuobaidah M, Fu H (2013) Structure and adsorption properties of sewage sludge-derived carbon with removal of inorganic impurities and high porosity. *Bioresour Technol* 142:209–217